PERGAMON

Scripta mater. 42 (2000) 603–607

Scripta MATERIALIA

www.elsevier.com/locate/scriptamat

ELECTRIC CHARACTERIZATION OF (Sr, Sr-Ba, Ba) M-TYPE FERRITES BY AC MEASUREMENTS

A. Huanosta-Tera[a], R. de Lira-Hueso[b], O. Pérez-Orta[b], S.A. Palomares-Sánchez[c], S. Ponce-Castañeda[b] and M. Mirabal-García[c]

[a] Instituto de Investigaciones en Materiales, UNAM, 04510 México, D.F., México [b] Facultad de Ciencias, Universidad Autónoma de San Luis Potosí, 78 000 San Luis Potosí, S.L.P., México [c] Instituto de Física, Universidad Autónoma de San Luis Potosí, 78 000 San Luis Potosí, S.L.P., México

(Received August 19, 1999)
(Accepted January 20, 2000)

Keywords: Sintering; Impedance spectroscopy; Ferrites; Electronic conductivity

Introduction

Considering the electrical conductivity in ceramics, necessary reference should be given to dynamic processes occurring as a function of frequency and temperature [1]. Although the most immediate interest in ferrites lies in their magnetic properties, technological applications require a wider knowledge of general physical properties as well. This is especially applicable when the materials are studied as a function of composition or when adding different modifiers.

In this report, we present results of the ac and dc electric characteristics of a family of magnetoplumbite-type hexaferrites, where Ba gradually substitutes Sr in the $Ba_xSr_{1-x}Fe_{12}O_{19}$ compound ($0 \leq \times \leq 1$). The results were determined over a wide range of frequencies and temperatures.

Experimental Procedures

(Ba,Sr)-M-type ferrites were prepared by the ceramic method. The basic powders $BaCO_3$, $SrCO_3$ and Fe_2CO_3 were mixed stoiquiometrically to obtain $Ba_xSr_{1-x}Fe_{12}O_{19}$, (x=0.0, 0.25, 0.50, 0.75 and 1.0). High purity powders from Strem Chemicals were used. In the preparation of the specimens, all the constituent oxide powders were mixed homogeneously by ball-milling in ethanol for two hours. After this, the resulting mixture was ground in air using a silicon nitride mortar in order to reduce the particle size. Powders were presintering at temperatures of 800°C during 2:45 hours. An initial ramp of 550°C/h was used. Polyvinyl alcohol was used as a binder and samples of different sizes were pressed as discs by applying a pressure of 3.5 Tons/cm^2. For the sintering process of the samples a temperature ramp of 300°C/h and a dwell of 600°C during one hour and a ramp of 300°C/h up to 1200°C for one hour were applied. Electrical conductivity measurements were made in the frequency from 5Hz to 13MHz range, using an HP4192A Impedance Analyzer. Gold electrodes were previously fabricated on the opposite faces of all specimens by means of small strips of gold foil and organogold paste. Using a vertical furnace with a proper temperature control, the frequency measurement were carried out from room temperature up to 773K. The applied voltage was 1.0V, in every case. In a totally independent experiment, the Curie temperature was determined from measurements of the thermal variation of

PII: S1359-6462(99)00409-1

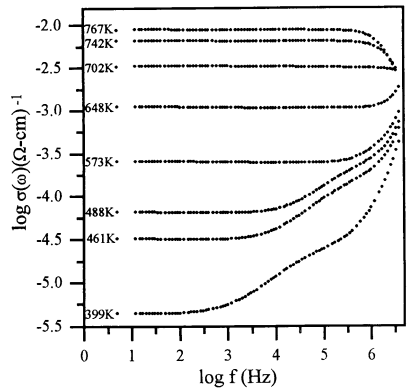

Figure 1. Typical frequency dependent behavior of $\sigma_t(\omega)$, at different temperatures, for the composition x = 0.50.

magnetic permeability [2]. Micro-structural studies were also carried out by atomic force microscopy. Results reveal a slight difference in the grain size, which ranges from 0.220 μm for x=0.5 to 0.349 μm for x-1.0. Those values were calculated using the Scherrer formula. Studied compositions include samples of $Ba_xSr_{1-x}Fe_{12}O_{19}$ with x = 0.0, 0.25, 0.50, 0.75 and 1.0.

Results and Discussion

There is not yet a fully acceptable explanation with regard to the microscopically involved processes occurring in the dynamic conductivity of dielectric systems, several approaches [3,4,5,6] have been given. However, as a matter of fact, it has been accepted that the dispersive behavior of the total experimental ac conductivity ($\sigma_t(\omega)$), in a very broad variety of materials, follows the relation

$$\sigma_t(\omega) = \sigma(0) + A\omega^s \tag{1}$$

proposed by Jonscher [3], where the first term $\sigma(0)$ is considered frequency independent; as $\omega \rightarrow 0$ it can be identified with the dc conductivity. The purely dispersive component $A\omega^s$ describes ac phenomena. A and s ($0 < s < 1$) are temperature and frequency dependent parameters [7]. The total conductivity can be obtained by $\sigma_t(\omega) = gfY'$, where Y' is the real part of the admittance ($Y = Y' + iY''$) and gf is a geometrical factor. Raw data consists in the real and imaginary parts of impedance, thus Y' can be calculated by $Y' = Z'/\{(Z')^2 + (Z'')^2\}$.

We have worked out $log\sigma_t(\omega)$ vs. $logf$ curves; they follow the mathematical relation (1), although they also exhibit an additional power law component ($A_2\omega^{s2}$) . Relation (1) should then be written as $[\sigma_t(\omega) = \sigma(0) + A_1\omega^{s1} + A_2\omega^2]$. That means that at low frequencies an almost frequency independent region is present followed by two dispersive regions, the first one ($A_1\omega^{s1}$) of which was assigned to dispersion in the grain boundaries; whereas the one at high frequencies ($A_2\omega^{s2}$) is associated to dispersion from the grains. This asseveration will be discussed later. Typical curves are exhibited in Figure 1 for x = 0.5.

The prefactors A_1 and A_2 follow a quasi-linear type Arrhenius behavior. The associated activation energies vary decreasingly from 1.87eV (x = 0.0) to 1.0 eV (x = 1.0), with a minimum value of 0.54eV (x = 0.5). The s_1 and s_2 parameters have a maximum value of 0.8, decreasing with increasing temperature, with the particularity that the s_2, from the bulk, has a change of slope at a temperature close to T_C. This is a non-typical result. The explanation may be associated with physical process occurring close to T_C. With regard to this, T_C has been obtained by continuously recording the initial permeability

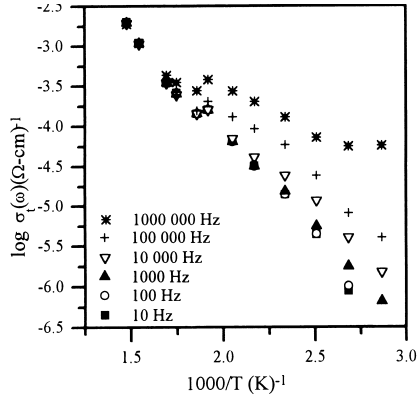

Figure 2. Temperature dependence of $\sigma_t(\omega)$ for samples with x = 0.50.

as a function of temperature [8]. In Table 2 we show all determined T_C values. The transition temperature changes as the Ba content increases and it is observed that there is a minimum at the composition x = 0.50.

At high temperatures, below T_C, the normal spin configuration in the magnetic system barely interferes with the already working charge transport mechanism in the sample. Increasing temperatures produce thermal fluctuations of spin configuration and induce thermal vibrations, which tend to misalign the magnetic moments. Thus, electron-lattice interactions become important and they can modify long range carrier mobility and forward-backward activity as well. This type of interaction is particularly effective at high frequencies bearing the important consequence that the observed change of slope appears, Figure 1. The dispersive behavior which is observed at frequencies higher than 10^7 Hz is due to the resolution limit of the measurement equipment.

To display the frequency and temperature dependence of the total conductivity we have plotted $log\sigma_t(\omega)$ against $1000/T$ at fixed frequencies, Figure 2. There seems to be an Arrhenius behavior in two temperature intervals with different activation energies. At high temperatures all conductivity curves seem to be convergent. Such a conductive regime tends to correspond to the σ_{dc} component. At these temperatures creation of intrinsic defects could be expected. Therefore, in the high temperature side of Figure 2, the steep slope reflects the energy (E_{dc}) which is required both to create and to move defects. Major amounts of charge carriers can jump toward vacant sites, thus long-range process dominates this stage.

At low temperatures a separation occurs in the low frequency conductivity from that of the high frequency regime. At high frequencies the period of time available is too short. That means that the probability of the charge carrier to jump back to its initial site increases, implying that the correlated forward-backward hopping of the charge carriers are responsible for the high frequency dispersion. In the low temperature range, for all the studied compounds, the activation energy, E_{ac}, decreases gradually at increasing frequencies, Table 1. An increase in the magnitude of the ac conductivity is observed as the frequency rises. It can be appreciated in Figure 2. This is a consequence of the fact that the required energy correlated with forward-backward hopping is only a fraction of the energy necessary to activate long-range diffusive conduction.

Close to room temperature the experimental information in the impedance plane seems to be a fraction of a semicircle, but as the temperature rises the curves become a well defined combination of a couple of arcs. A typical family of Z'' vs. Z' curves are shown in the inset of Figure 3, at selected temperatures. Each one of the arcs can be associated with the electrical response of a region in the sample. A simple equivalent circuit proposed to simulate the electrical behavior can be constructed by

TABLE 1
Activation Energies for Pure ac Behavior

Frequency (kHz)	E_{ac} (eV) x = 0.00	E_{ac} (eV) x = 0.25	E_{ac} (eV) x = 0.50	E_{ac} (eV) x = 0.75	E_{ac} (eV) x = 1.00
10^{-2}	0.57	0.85	0.56	0.59	
10^{-1}	0.63	0.84	0.54	0.56	
1	0.53	0.56	0.49	0.47	
10	0.45	0.40	0.40	0.29	0.30
10^{2}	0.37	0.31	0.36	0.18	0.18
10^{3}	0.16	0.17	0.18	0.11	0.13

two parallel *RC* loops connected in series. The first one (R_1C_1) corresponds to high frequency data and the second one (R_2C_2) to the low frequency region. Resistivity values (R) can be obtained at the corresponding intersection on the low frequency side of the arcs occurring in the impedance plane. This task was assisted by the NLLS fitting routine by Boukamp [9]. The associated capacitance values on each arc can be used as a criterion to assign the physical origin of the electrical response on the whole impedance curve [10]. Each semicircle holds the relationship $2\pi f_{max}RC = 1$, where f_{max} is the frequency on the maximum of the impedance curve and R is the corresponding calculated resistance value. From this, capacitance values on the high frequency arc (C_1) are in the order of pF, which allows the conclusion that response is coming from the grains of the sample, i.e. the bulk. At the low frequency side, C_2 values are in the order of nF. This is an accepted value for grain boundary phenomena [10]. The R-values were plotted in a $log\sigma$ against $1000/T$ format, where $\sigma = gf/R$. In Figure 3 we only show results for bulk conductivity (σ_g). For every studied sample, conductivity data fit closely to a linear Arrhenius behavior. Although the main observation here is that the variation of the Ba/Sr ratio modifies the conductivity mechanism leading to a continuous decrease in conductivity as the Ba/Sr ratio diminishes. The activation energies corresponding to the bulk E_{ga} and grain boundary E_{gb} are presented in Table 2.

C_1 has also been used to calculate the dielectric constant (ϵ') of all compounds, $\epsilon' = C_1gf/\epsilon_o$, where ϵ_o is the dielectric constant of free space). The largest value for ϵ' corresponds to the x = 0.0 sample ($\epsilon' \approx 1300$), decreasing as the barium content increases, around 100 for x = 1.0.

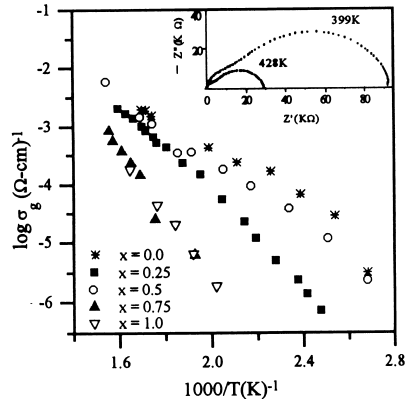

Figure 3. Temperature dependence of bulk conductivity for all studied compounds. The inset shows a family of typical impedance plots, at selected temperatures, for the composition x = 0.50.

TABLE 2
All Involved Activation Energies and T_C Values

x	E_{dc} (eV)	E_g (eV)	E_{gb} (eV)	E_t (eV)	T_C (K)
0.00	0.60	0.42	0.43	0.67	725
0.25	0.68	0.77	0.71	0.78	719
0.50	0.53	0.54	0.43	0.69	716
0.75	0.79	0.90	0.92	0.79	718
1.00	0.86	1.05	1.11	1.166	725

The relationship $\omega_{max}RC = 1$ can also be used to calculate the electrical conductivity relaxation time $\tau = 1/(2\pi f_{max})$, where f_{max} is the frequency at the maximum of the impedance semicircles. This is a proper parameter to measure the time that an electron takes to jump a distance equal to the separation between electronic defects. We have found $log\tau_\sigma$ as a function of $1000/T$ (not shown). In this case the behavior of τ_σ is distributed in a narrow strip which covers jump times from 10^{-3} s to 10^{-7} s. In general, it was possible to calculate the activation energy E_τ in all cases. All these values are also shown in Table 2.

Conclusions

The frequency dependence of the dynamic conductivity follows a power law behavior, with the particularity that the dispersive component includes two terms. One of them stems from the grains ($A_2\omega^{s2}$), and the other one from the grain boundaries ($A_1\omega^{s1}$). One interesting result refers to the temperature dependence of the s_2 parameter. The change in slope related to the s_2 parameter must reflect temperature activated electron-lattice interactions close to T_C. Temperature dependent dynamic conductivity plots were used to extract the dc component as well as all involved activation energies. Separation of the ac component, particularly at low temperatures, was also possible throughout those plots.

Acknowledgments

This project was supported by CONACyT (grant Nr. 485100-5-2232P), and DGIA-UNAM, México. The authors are also indebted to M. Kempton Padmore for technical support.

References

1. J. R. Macdonald, ed., Impedance Spectroscopy, John Wiley, New York (1987).
2. E. Cedillo, J. Ocampo, V. Rivera, and R. Valenzuela, J. Phys. E. Sci. Instrum. 13, 383 (1980).
3. A. K. Jonscher, Nature. 267, 673 (1977).
4. D. P. Almond, G. K. Duncan, and A. R. West, Solid State Ionics. 8, 159 (1983).
5. K. Funke, Prog. Solid State Chem. 22, 111 (1993).
6. S. R. Elliot, Solid State Ionics. 27, 131 (1988).
7. F. Salam, J. C. Guintini, S. Sh. Soulayman, and J.V. Sanchetta, Appl. Phys. A. 63, 447 (1996).
8. A. Globus, J. Phys. 38, C1–1-15 (1977).
9. B. A. Boukamp, Equivalent Circuit, University of Twente, Department of Chemical Technology, Netherlands.
10. J. T. S. Irvine, D. C. Sinclair, and A. R. West, Adv. Mater. 2, 132 (1990).